

PAPER • OPEN ACCESS

Friction dissipation in reciprocating internal combustion engines: cam tappet contact

To cite this article: P Sansone and M Lavella 2021 *IOP Conf. Ser.: Mater. Sci. Eng.* **1038** 012041

View the [article online](#) for updates and enhancements.



240th ECS Meeting ORLANDO, FL

Orange County Convention Center Oct 10-14, 2021



Abstract submission due: April 9

SUBMIT NOW

Friction dissipation in reciprocating internal combustion engines: cam tappet contact

P Sansone¹ and M Lavella^{1,2,3}

¹ Politecnico di Torino - DIMEAS Dipartimento di Ingegneria Meccanica e Aerospaziale, Corso Duca degli Abruzzi, 24, 10129 Torino, Italy

² Università degli Studi di Bergamo – DIGIP Dipartimento di Ingegneria Gestionale, dell'Informazione e della Produzione, viale Marconi, 5, 24044 Dalmine (BG) – Italy

³ Corresponding author's e-mail address: mario.lavella@unibg.it

Abstract. The interest towards fuel consumption reduction in reciprocating internal combustion engines has achieved a key role starting from the first energy crisis during the 70's. Even if in alternate phases, such interest had further increased during the following years assuming a fundamental role in the last years. The reason lies in the introduction of regulations that limit the emissions of carbon dioxide, as it belongs to the family of greenhouse gasses. A reduction of the friction dissipation reflects directly on consumption reduction and consequently in an improvement of emissions. The main goal of this research is to model the friction dissipation at the cam tappet interface. In this research an analytic model is proposed, it allows to estimate the dissipation due to friction with a complexity appropriate to that of the design phase and which allows to select between different design solutions in order to optimize the efficiency of the cam tappet interfaces. Model results are coherent with experimental results reported in literature.

1. Introduction

The efficiency, and consequently the fuel consumption, of Reciprocating Internal Combustion Engine (RICE) has always been one of the main interests of designers. However, during some historical periods this interest was stronger. Moreover, this was also the driving force to introduce important changing in design of RICE. After the first energy crisis in 1973 the focus in designing RICEs have been moved on consumption more than ever. In this period the attention to consumption derived mostly from the economic aspect related to it, lately with the introduction of regulations that limit the emissions of greenhouse gasses, the focus has been turned mostly on the resulting environmental impact.

Many studies about losses in RICEs were done, the Massachusetts Institute of Technology states that the 74% of the fuel energy put in a RICE is dissipated by the same [1], another study affirms that the 11.5% of the fuel energy in a RICE is used to overcome friction, of which the 15% in the valvetrain [2]. The same percentage of loss (15%), in respect to the total friction losses in the RICE, was found in another study [3]. Moreover, this research reports that the percentage of friction loss in the valvetrain at low speed increases up to 40% of the total friction loss [3]. The increasing in friction loss with decreasing of engine speed was also confirmed from an experimental test in which the actual friction torque applied to the camshaft was measured at different speeds, noting that the friction torque increases with decreasing engine speed [4].



The engine speed has a major influence in generating stresses and wear at the cam tappet interface [5] moreover it was found that the 70% of the valvetrain's friction losses occurs at the cam tappet interface [6]. Since a large quantity of friction loss in the valvetrain is localized at the cam tappet interface, reducing the friction coefficient at the same is crucial. It was found that some kind of coatings decrease the friction coefficient and increase the wear resistance of the cam and tappet surfaces [7], [8]. A significant friction reduction of over ten up to thirty percent was achieved from micro texturing and amorphous carbon coating, respectively [9]. However coatings have also important implications on fatigue [10], [11], [12].

The aim of this work was to develop an analytic model, suitable for the design phase, able to evaluate the friction dissipation at the cam tappet interface. Consequently, this model has to be able to quickly and accurately estimate the amount of fuel energy wasted for friction in the valvetrain in order to make a choice between different design solutions. The timing apparatus is fundamental for the engine to work since it controls the fluxes into the combustion chamber and outward. Different design solutions can be adopted for the motion transmission, belts, chains, rods and rockers, although numerous solutions are found, the cam tappet interface is always responsible for friction dissipation. The model describes the relations between geometry, kinematics and dynamics of the two components and the entity of friction dissipation determined by using the Amontons-Coulomb friction model. This model becomes really useful during the design phase in which different design solutions have to be compared in relation with their friction dissipation. Therefore, it can quickly evaluate the constructive solution that gives better results in terms of carbon dioxide emissions. Results showed that the friction torque decreases when the engine speed increases according to the experimental tests of literature [4]. Moreover, the total moment calculated with the model assumes the same trend measured [4]. The percentage of fuel power wasted for friction was found to be the same as estimated in other analysis [2]. The results agreement means that the model developed is a good instrument of evaluation, moreover it doesn't need the amount of time typically required for experimental tests or numerical solutions.

2. Nomenclature

$b(\alpha)$	Arm of the forces perpendicular to the tappet	M_i	Momentum of the inertial force
E_{diss}	Dissipated energy by friction	M_{tot}	Total momentum
F_f	Friction force	m_{tap}	Mass of the tappet
$H(\alpha)$	Arm of the forces parallel to the tappet	m_{valve}	Mass of the valve
$h(\alpha)$	Lift law	N_e	Spring force
$\dot{h}(\alpha)$	Velocity of the tappet	N_i	Inertial force
$\ddot{h}(\alpha)$	Acceleration of the tappet	r_0	Radius of the base circle of the cam
k	Spring stiffness	α	Camshaft rotation
m_{alt}	Masses under alternating motion	μ_{CP}	Coefficient of friction
M_e	Momentum of the spring force	ω	Angular velocity of the cam
M_f	Momentum of the friction force		

3. Modelling methodology

The model was developed considering an OverHeadCamshaft system where the cam operates directly on the tappet surface figure 1. It is important to specify that at this point of the analysis the geometry and properties of the cam and the tappet have been set, this means that the lift laws determined by the cam profile are known. In this analysis a two centres cam was adopted, but the model is not restricted to this cam profile. By knowing the lift laws and the geometries, all the forces at the cam tappet interface are calculable.

If gravitational force is neglected, as well as reactions at the tappet's housing, three forces act on the tappet, friction force, inertial force and spring force figure 1. The friction force acting at the tappet-housing interface was neglected because the normal load acting at the tappet-housing interface would be approximately the friction force generated at the cam tappet interface, therefore with a friction coefficient of 0.1 the resultant friction force at the tappet-housing interface would be ten times smaller

than the friction force acting at the cam-tappet interface. The friction force at the cam-tappet interface was calculated by adopting the Amontons-Coulomb's friction model and the friction coefficient was considered constant. This hypothesis was used only for computations and not restricts the model, more general results can be obtained using the Stribeck curve. Moreover, the camshaft angular velocity was considered steady. The goal was to calculate the friction moment and obtaining the energy dissipated during an engine cycle:

$$M_f = (kh(\alpha) + m_{alt}\ddot{h}(\alpha))\mu_{CP}(r_0 + h(\alpha)) \tag{1}$$

$$E_{diss} = \int M_f d\alpha \tag{2}$$

Where M_f is the momentum of the friction force; k is the spring stiffness; $h(\alpha)$ is the lift law of the tappet as a function of the camshaft rotation (α); $\dot{h}(\alpha)$ is the acceleration of the tappet; μ_{CP} is the friction coefficient; r_0 is the radius of the base circle; E_{diss} is the energy dissipated by friction.

The spring force (N_e) can be directly determined by knowing the stiffness of the spring and the lift law:

$$N_e = kh(\alpha) \tag{3}$$

The cam's profile generates an acceleration on the tappet, this acceleration is applied on different masses (m_{alt}), mainly on the tappet (m_{tap}), valve (m_{valve}) and the spring (m_{spr}). Since the spring is compressing/elongating it follows that different points on the spring's length undergo different acceleration. The acceleration will be maximum at the tappet and equal to zero at the spring housing. To take account of this, assuming that the acceleration trend along the spring is linear, just a fraction of the total spring's mass ($1/2 m_{spr}$) is considered for the calculation of the inertial force:

$$m_{alt} = m_{tap} + m_{valve} + \frac{1}{2}m_{spr} \tag{4}$$

$$N_i = m_{alt}\ddot{h}(\alpha) = (m_{tap} + m_{valve} + \frac{1}{2}m_{spr})\ddot{h}(\alpha) \tag{5}$$

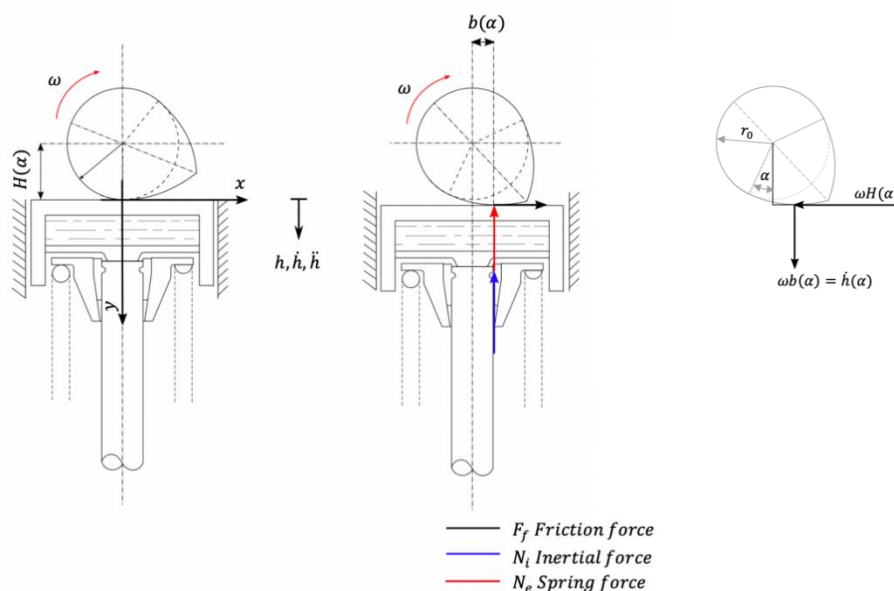


Figure 1. Schematization of the forces exerted at the cam-tappet interface.

Since a normal load is present, as well as a relative motion, it follows that friction force is generated. By adopting the Amontons-Coulomb's friction model, the friction force can be determined as follows:

$$F_f = (N_e + N_i)\mu_{CP} = (kh(\alpha) + m_{alt}\ddot{h}(\alpha))\mu_{CP} \quad (6)$$

The whole complexity of the phenomenon is incorporated in the friction coefficient which would be described by appropriate functions determined experimentally or throughout other models. Once all the forces acting at the cam-tappet interface are found, the moments exerted on a cam can be evaluated. Since all the geometries are set, the lever arm with which every force act in respect to the cam's rotational centre can be found. The hypothesis to determine the lever arms is that every force is exerted at the geometric contact line. The lever arm with which the friction force acts is:

$$H(\alpha) = r_0 + h(\alpha) \quad (7)$$

The inertial force and the friction force act on the cam with a lever indicated as $b(\alpha)$, this can be found by adopting the conjugate profile theory. By equating the velocities perpendicular to the tappet surface, it follows:

$$b(\alpha) = \frac{\dot{h}(\alpha)}{\omega} \quad (8)$$

In the end it is possible to obtain the total moment exerted on a cam:

$$M_{tot} = M_e + M_i + M_f = kh(\alpha)\frac{\dot{h}(\alpha)}{\omega} + m_{alt}\ddot{h}(\alpha)\frac{\dot{h}(\alpha)}{\omega} + (kh(\alpha) + m_{alt}\ddot{h}(\alpha))\mu_{CP}(r_0 + h(\alpha)) \quad (9)$$

4. Results

The model was applied to a two centers cam profile characterized by the parameters listed in table 1, the angular velocity of the cam was considered constant as well as the friction coefficient ($\mu_{CP} = 0.1$ steel-lubricated steel). Kinematics characteristics of this profile (lift laws, velocity and acceleration) are reported in figure 2. To fully understand the characteristics of the cam-tappet system some notable cases were identified as a simplification of general model, such as negligible inertial forces and negligible elastic force. These allowed to consider every aspect of the phenomena ruling the system.

Table 1. Reference parameters.

Parameters	Values
Angular velocity of the cam	2500 rpm
Base circle array	9.2 mm
Second circle array	39 mm
Second circle angle	32°
Spring stiffness	45 kN/m
Friction coefficient	0.1
Valve's mass	0.0640 kg
Spring's mass	0.0770 kg
Tappet's mass	0.0390 kg

With regard to the general model, the forces acting at the cam-tappet interface (elastic, inertial and friction forces) were calculated and illustrated in figure 3. It is possible to observe how the normal load (spring force + inertial force) exhibit discontinuity that is more evident at higher velocities (figure 4).

This is because of the inertial force that has the same characteristic of acceleration profile (figure 2) and is a consequence the irregularities of cam profile adopted. The parametrization over the angular velocity shown in figure 4, highlights that the normal load tends to become continuous with the decreasing angular velocity of the cam, normal load and friction force are near to a continuous function at 500 *rpm*. After calculating the single forces acting at the cam-tappet interface and the single moments, the total moment was determined (figure 5).

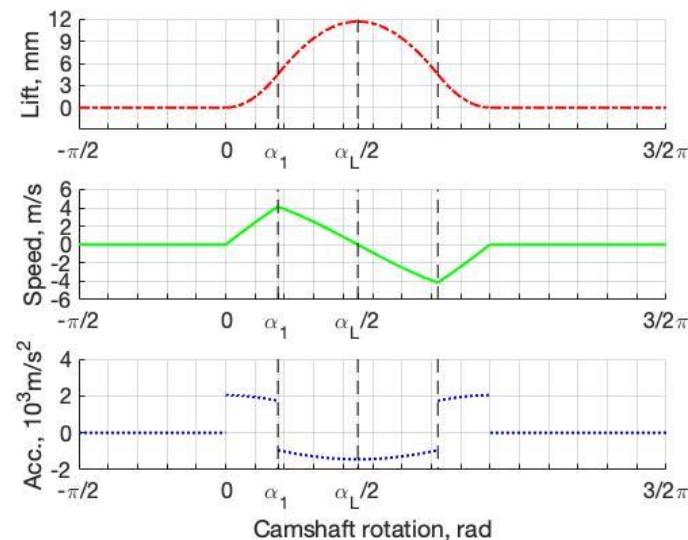


Figure 2. Lift laws for a two centers cam described by the parameters shown in table 1.

Analogously to the forces, the trend of total moments tends to become more continuous functions with the decreasing angular velocity of the cam, at 500 *rpm* the trend is near to continuous. Observing the forces and moments trend at 1500 *rpm*, it can be observed that this approximation can be extended up to camshaft rotation speed of 1000 *rpm* which corresponds to 2000 *rpm* of crankshaft speed. In other word, this approximation can be extended to the majority of industrial engines. The friction moment was subsequently integrated over a cycle, in order to obtain the value of friction dissipation resulting from a cam in one engine cycle. In figure 6 are reported the trends of the cam's dissipation as a function of the angular velocity of the cam, parameterized on different friction coefficients. It has to be highlighted that no preload of the spring valve was considered in the previous analysis. Considering a linear spring with a preload, a lower stiffness can be used. The reason is that the preload generates a normal load at the cam-tappet interface, guaranteeing the one-side contact condition with a lower stiffness of the spring. Since the one-side contact condition between cam and tappet must be verified, the normal load at the cam tappet interface must always be negative (green dashed line figure 3), according to the adopted sign convention. To get comparable results to those of the case without spring preload, the same condition of minimum normal load was considered in both cases (-60 *N*). In figure 7 the illustrates the force's trends by using a preload of 3 *mm* and a spring stiffness of 27 *kN/m*, the one-side contact condition is verified with a minimum normal load of -60 *N*, that is same minimum normal load imposed at higher stiffness. A preload on the spring affects the normal load on the cam-tappet interface and consequently the entity of friction dissipation. In order to evaluate the dependence of friction dissipation on spring preload, figure 8 reports model results with and without preload. This figure highlights that the friction dissipation with spring preload (blue lines) are always lower than that without preload (red lines).

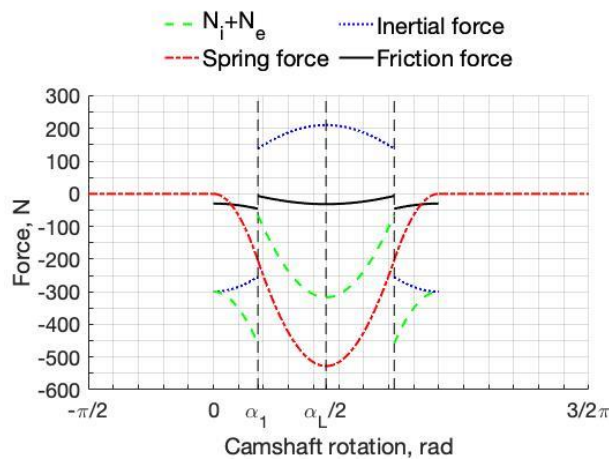


Figure 3. Force's trend for a spring-based cam-tappet system without spring preload.

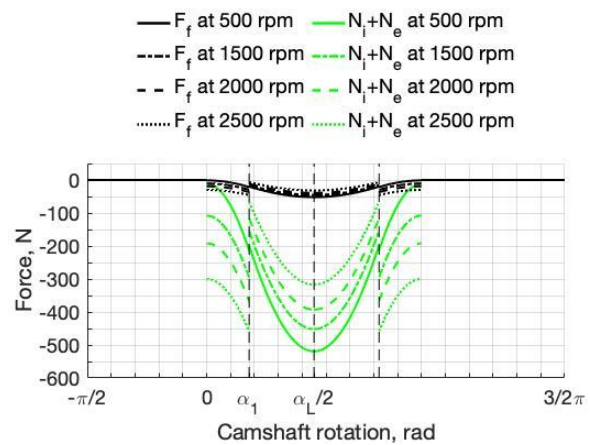


Figure 4. Force's trend for a cam-tappet system at multiple velocities.

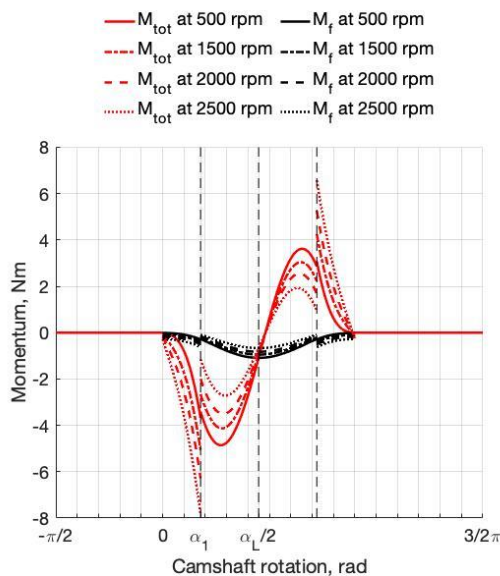


Figure 5. Total moment trends for a cam-tappet system parameterized on angular velocities.

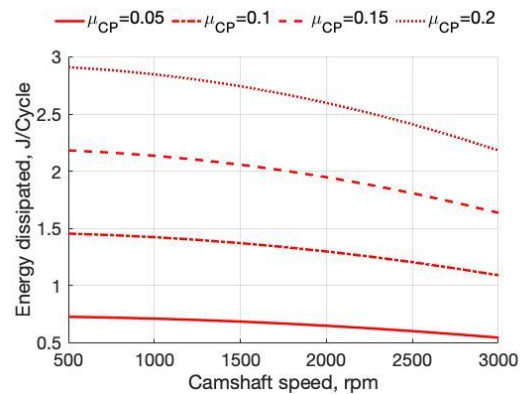


Figure 6. Friction dissipation trends for 1 cam in 1 cycle, parameterized for friction coefficient.

In many scenarios and many engine applications the engine speed's regime is very low, e.g. diesel engines in marine or tractors applications. In all cases characterized by lower velocities, inertial forces can be neglected and the normal load (sum of inertial loads and spring force) can be identified with the spring force. Figure 9 shows the model results in terms of force at cam-tappet interfaces when the inertial force can be neglected. In this case, the normal load, friction force and relative moments, reported in figure 10, exhibit continuous trends.

In contrast, the case with a negligible spring stiffness (spring force much lower than inertial one) was analyzed. This may seem like an abstract assumption, but it is appropriate to model a Desmodromic valvetrain system. In these systems, the closing stroke of the valves is operated by a second cam and not from a spring. Although a spring is a component of the system, it has a negligible effect on the contact

force. Removing the spring effects, model results displays the forces' trends reported in figure 11. In this case the normal load is equal to the inertial force and it reflects all discontinuity of the lift law (two centers cam profile).

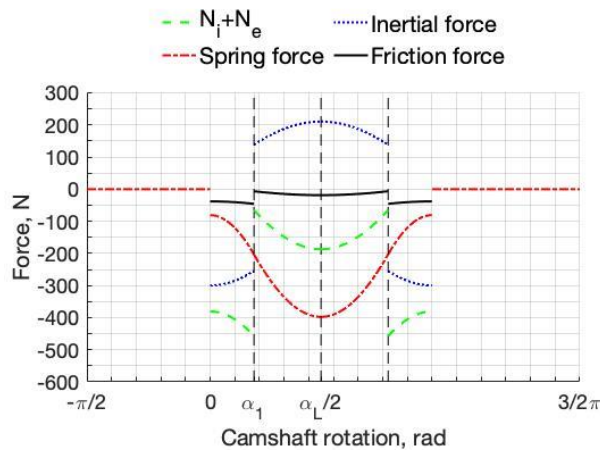


Figure 7. Force's trend for a spring-based cam-tappet system, spring preload 3 mm and spring stiffness 27 kN/m.

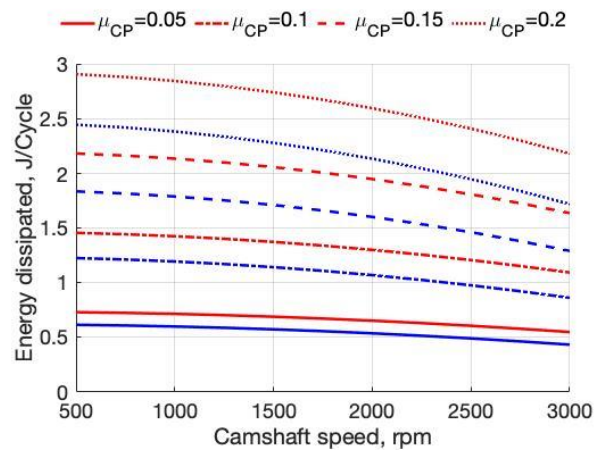


Figure 8. Friction dissipation trends for 1 cam in 1 cycle, parameterized for friction coefficient, preload (blue), no preload (red).

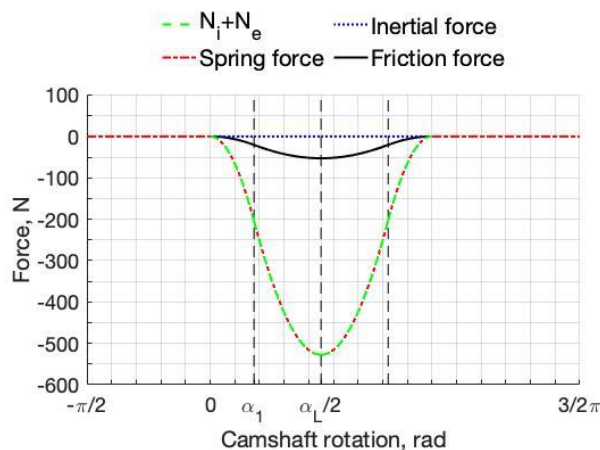


Figure 9. Forces' trends for slow engines (negligible inertial forces).

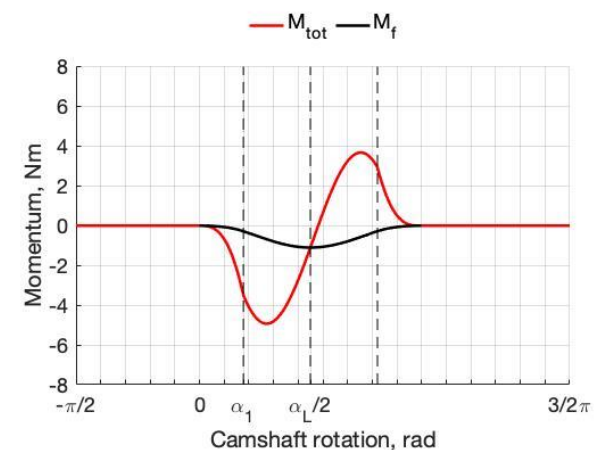


Figure 10. Total moment's trend for slow engines (negligible inertial forces).

Model results of total and friction moments are shown in figure 12, while the relative dissipated energy during one engine cycle is illustrated in figure 13. This shows the trends of friction dissipation (1 cam on 1 cycle) as a function of the angular velocity of the camshaft parameterized on the friction coefficient. Figure 13 indicates that friction dissipation increases with the increasing of the angular speed, because of inertial force is directly related to the angular velocity of the shaft.

The model developed was also applied to a real case in order to evaluate friction loss at cam-tappet of a car in service in a short trip. Through an OBD instrumentation were acquired engine regime, distance travelled and travel time of a car engine traveling in a suburban road clear of traffic. Figure 14

reports engine regime as a function of travel time. The car was a small-car equipped by a 3-cylinder engine with 4 valves for each cylinder (12 valves).

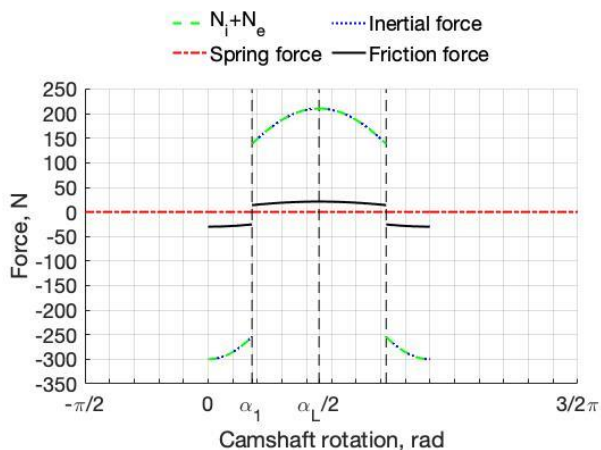


Figure 11. Forces' trends for the simplification of a desmodromic system.

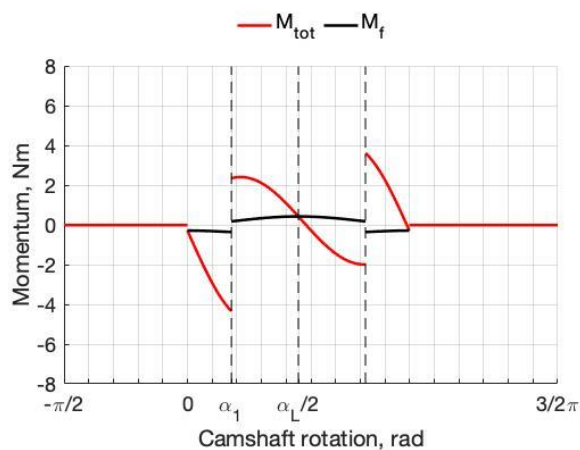


Figure 12. Total moment's trends for the simplification of a desmodromic system.

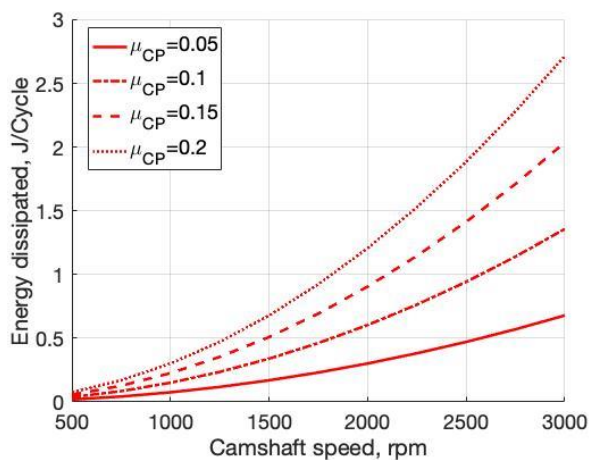


Figure 13. Friction dissipation trends for 1 cam in 1 cycle, parameterized for friction coefficient μ_{CP} , negligible spring force.

The fuel consumption released by car manufacturer was a 4.4 liters per 100 km. Based on travelled distance of 11 km the fuel consumed was 0.484 l in 15 minutes. Through the gasoline characteristics was estimate the energy provided by fuel to the engine. Since the calorific value was 44 MJ/Kg and the density of the gasoline is 0.75 kg/l, the total fuel energy consumed amounts to 15.97 MJ. Through the friction loss at each cam cycle (results shown in figure 8) and time history of engine regime, the total friction energy loss of all cam tappet interfaces. Since the average engine speed is 2250 rpm, the camshaft speed is 1125 rpm on average. At this camshaft speed, each cam has a friction loss of about 1.4 J/cycle (figure 6 $\mu_{CP} = 0.1$). Considering travel time and the average camshaft's speed, the total cam's cycles during the travel was about 16900 cycles. Consequently, the total friction loss by all cam-tappet interfaces amounts at 284.4 kJ which represent almost the 2% of the total fuel energy.

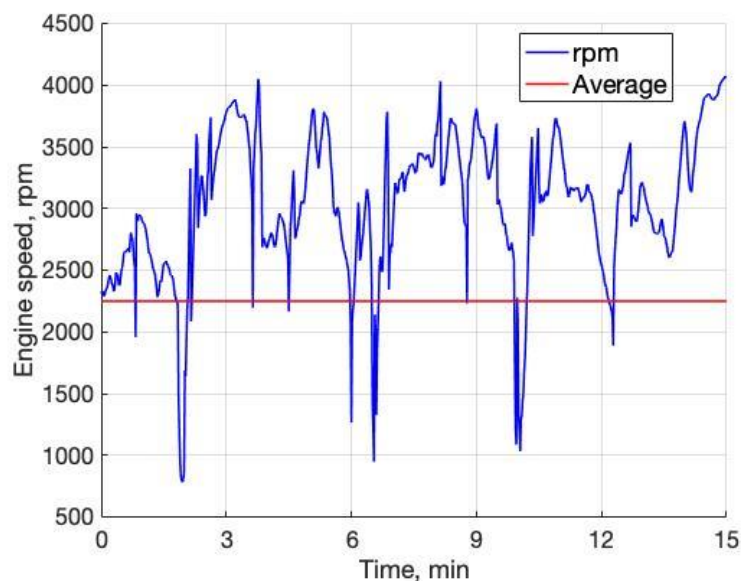


Figure 14. OBD's data.

5. Discussion

Forces and moments acting on the cam-tappet system were evaluated applying a constant friction coefficient to the developed analytic model. This assumption was not strictly necessary, it was only used to better illustrate and discuss effects on dissipation of this and other parameters. On the contrary, in order to have a good prediction capability of model, the friction coefficient have to be described by more complex function because of the friction coefficient includes in itself the complexity of interfaces phenomena. Therefore, friction coefficient should be described by appropriate ways based on other models or experimental data. In this application a more appropriate model to describe friction coefficient for friction coefficient is the Stribeck curve. However, by means of a good description of friction coefficient all design actions on contact interfaces (e.g. coatings, lubricants) can be described, included fretting [13] impact dissipation at valve-housing interface. Coatings have important implication on contact parameters of interfaces [8],[9], and fatigue [10], [11], [12].

Optimizations and comparison of constructive solution including lubricants can be based on this model in order to quickly evaluate the effects on friction dissipations and deliver a better design. With reference to the illustrated results, an example was the analysis of preload effect on the spring, figure 8. In that case, a right combination of spring stiffness and preload reduced the normal load on the contact interface and consequently friction dissipation. Moreover, the model can be also useful to identify more interesting design parameters to effective to optimize friction dissipations. Model results may be used to compare the widespread constructive solution based on spring returned system (spring returned lift) with desmodromic systems (cam returned lift). Figure 15 compares the dissipated energy as a function of camshaft speed for these alternative solutions. Spring returned system appears more convenient at high rotational engine regimes, particularly in proximity of the maximum rotational regime of that specific engine. In contrast, the desmodromic system was more convenient at low regimes. In terms of dissipation, the choice between these two design solutions depends on the usual working regime (*rpm*) of the specific engine compared to the maximum regime design of the same engine. A desmodromic system should be used in engines that work mainly at low regimes; design solutions are equivalent for engines that usually work at medium-high regimes; spring returned system is the better choice for engines that mainly work at high regimes. Because of the stiffness of spring depends on the maximum

rotation velocity of the engine, the angular velocity at which these two dissipations are equivalent depends on the maximum regime at which was designed the specific engine. On the other hand, dissipation results shown for desmodromic system were obtained by neglecting the mass of any rockers. In desmodromic systems, these components cannot be avoided. However, rockers can be easily included in this model adding their inertial actions. This induces an increasing in normal load applied on the contact interfaces. Thus, friction dissipation curve of desmodromic system increase its rate. Consequently, the equivalence point of these two dissipation curves move to lower angular velocities.

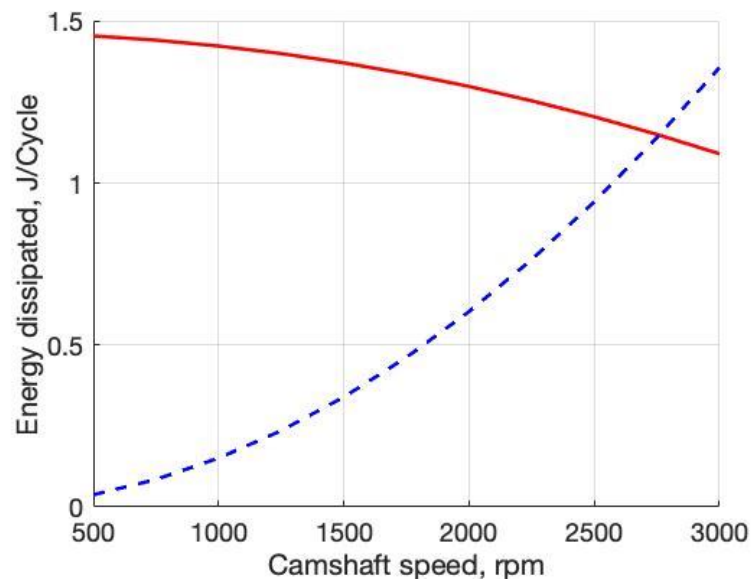


Figure 15. Spring returned system — versus desmodromic systems - - -.

The estimation of friction dissipation in cam-tappet interfaces of a car during a short trip service, 2% of fuel energy, was based on the fuel consumption released by the car manufacturer. This fuel consumption was evaluated by manufacturer in a service condition specified by regulations. The real fuel consumption during the specific trip and traffic conditions could be different. Therefore, a variation of this percentage has to be expected.

6. Conclusion

Considering an OHC timing system where the cam operates directly on the tappet surface, an analytic model of friction dissipation was developed. Friction forces were based on the Amontons-Coulomb friction model, therefore prediction capabilities of this model, depend on the accuracy of the coefficient of friction description at the contact interfaces. A good description (e.g using a Stribeck curve) allows to evaluate effects on friction dissipation of coatings, lubricants and surface finishing. Some remarkable case studies were identified neglecting inertial force or spring force. The case without inertial force allowed to analyze low speed engines. In this scenario the inertial force can be neglected until maximum regimes of 2000 rpm (crankshaft) so that this assumption could be applied to any industrial engine. In this applications friction dissipation was directly related to the spring characteristic. In contrast, the model of desmodromic timing apparatus can be found neglecting the spring force. Comparison of desmodromic timing apparatus with the spring returned system illustrates opposite trends of friction dissipation. Moreover, desmodromic system appears more convenient (in terms of dissipation) at low regimes. At medium high regimes desmodromic and spring returned systems are nearly equal demanding while spring returned system is more convenient at high regimes. With regard to spring returned system, friction dissipation was decreased by a good combination of spring design parameters

(stiffness and preload). Using OBD data of a small car, the friction dissipations of cam-tappet interfaces was correlated to fuel consumptions, approximately the 2% of the fuel energy is wasted to overcome friction at the cam-tappet interface. Model results agree with the results found in experimental measurements reported in [4], particularly the total moment as a function of camshaft angle and the trend of decreasing in friction dissipation predicted with the increasing in engine speed. This dissipation was also found [3].

Concluding, the proposed modelling methodology was founded on right assumption and is adequate to optimize the cam-tappet interfaces in terms of friction dissipations. This model is appropriate to engine design phase because of results agreement with experimental measurements, lower time-consuming than others and correlated to the design parameters. Future developments should be focused towards developing analogous models for other components such as rockers and rods timing apparatus, camshaft, crankshaft and others in order to obtain an optimized friction dissipated design of the entire engine. In other word a more environmentally friendly mechanical design of engines.

7. References

- [1] Bandivadekar A, Bodek K, Cheah L, Evans C, Groode T, Heywood J, Kasseris E, Kromer M and Weiss M 2008 *On the road in 2035* (Boston: Massachusetts Institute of Technology) p 23
- [2] Holmberg K, Andersson P and Erdemir A 2011 Global energy consumption due to friction in passenger car *Tribology international* **47** pp 223-25
- [3] Zhou Q, Shilling I and Richardson S H 2003 Prediction of total engine friction power loss from detailed component models *Tribological series* **41** p 764
- [4] Mufti R A and Priest M 2003 Experimental and theoretical study of instantaneous engine valve train friction *ASME* **125** p 635
- [5] Wenjang W, Haichao L, Mingjun Z, Zhanfeng G and Xiaolei Z 2018 Contact stress analysis of engine speed on cam tappet pair *U.S.B. Scientific Bulletin D* **80** p 54
- [6] Kushwahu M 2010 *Tribology and dynamics of engine and powertrain* Woodhead publishing limited (Sawston, Cambridge) p 565
- [7] Dobrenizki L, Tremmel S, Wartzack S, Hoffmann D C, Brögelmann T, Bobzin K, Bagcivan N, Musayev Y and Hosenfeldt T 2016 Efficiency improvement in automobile bucket tappet/camshaft contacts by DLC coatings-Influence of engine oil, temperature and camshaft speed *surface and coatings technology* **308** pp 364-72
- [8] Lavella M and Botto D 2011 Fretting wear characterization by point contact of nickel superalloy interfaces **271** pp 1543-51
- [9] Marian M, Weikert T and Tremmel S 2019 On friction reduction by surface modifications in the TEHL cam/tappet-contact-experimental and numerical studies *Coatings* **9** p 843
- [10] Lavella M and Botto D 2018 Fretting fatigue analysis of additively manufactured blade root made of intermetallic Ti-48Al-2Cr-2Nb alloy at high temperature *Mater.* **11** 1052
- [11] Arcieri E V, Baragetti S and Borzini E 2018 Bending fatigue behavior of 7075-aluminum alloy *Key Eng. Mater.* **774** 1
- [12] Baragetti S, Bozic Z and Arcieri E V 2020 Stress and fracture surface analysis of uncoated and coated 7075-T6 specimens under the rotating bending fatigue loading *Eng. Fail. Anal.* **112** 104512
- [13] Lavella M 2020 Partial-gross slip fretting transition of martensitic stainless steels *Tribology International* **146** 106163